

# New Results on $0\nu\beta\beta$ Decay from the CUORE Experiment

A. Campani<sup>1,2</sup> on Behalf of the CUORE Collaboration

<sup>1</sup>Dipartimento di Fisica, Università di Genova, 16146 Genoa, Italy

<sup>2</sup>INFN Sezione di Genova, 16146 Genoa, Italy

## Abstract

The Cryogenic Underground Observatory for Rare Events (CUORE) is the first bolometric experiment searching for neutrinoless double beta decay ( $0\nu\beta\beta$ ) that has successfully reached the tonne mass scale. The detector, located at the LNGS in Italy, consists of an array of 988  $\text{TeO}_2$  crystals arranged in a compact cylindrical structure of 19 towers. CUORE began its first physics data run in 2017 at a base temperature of about 10 mK and has been collecting data continuously since 2019, reaching a  $\text{TeO}_2$  exposure of 2 tonne-year in spring 2023. This is the largest amount of data ever acquired with a solid-state cryogenic detector, which allows for a significant improvement in the sensitivity to  $0\nu\beta\beta$  decay in  $^{130}\text{Te}$ . In this article, we present the analysis of new CUORE data, corresponding to  $\sim 1$  tonne  $\cdot$  yr  $\text{TeO}_2$  exposure. This analysis relies on significant enhancements to the data processing chain and high-level analysis. Combining the new data with the former data release, we find no evidence for  $0\nu\beta\beta$  decay and set a preliminary 90% credibility interval Bayesian lower limit of  $3.3 \cdot 10^{25}$  yr on the  $^{130}\text{Te}$  half-life for this process. In the hypothesis that  $0\nu\beta\beta$  decay is mediated by light Majorana neutrinos, this results in an upper limit on the effective Majorana mass of 75–255 meV, depending on the nuclear matrix element used.

*Keywords:* neutrinoless double beta decay, rare events, cryogenic detectors

DOI: 10.31526/LHEP.2024.516

## 1. INTRODUCTION

Our knowledge of neutrinos has a long history, but it remains incomplete and evolving. While the existence of nonzero neutrino masses is well established as a result of precision measurements of flavor oscillations [1], the absolute mass scale, the Dirac or Majorana nature of neutrinos [2], and the role of neutrino mass in cosmology [3] remain long-standing questions.

Searching for neutrinoless double beta decay ( $0\nu\beta\beta$ ) is currently the only realistic method of testing whether neutrinos are Majorana particles [4].

Double beta decay is a rare, second-order nuclear decay in which an initial nucleus ( $A, Z$ ) decays to a member of the same isobaric multiplet ( $A, Z + 2$ ) with the simultaneous emission of two electrons and two antineutrinos. The neutrinoless mode of such decay is a lepton-number-violating transition ( $\Delta L = 2$ ) whose observation would provide direct evidence of beyond Standard Model physics [5]. Furthermore, a discovery that neutrinos are Majorana particles would support the proposed theory of Leptogenesis to explain the present matter-dominated Universe [6].

In the simplest scenario,  $0\nu\beta\beta$  is mediated by the exchange of light Majorana neutrinos, and the rate of the process depends on the effective Majorana mass  $m_{\beta\beta}$ . The general interest has always remained focused on the neutrino mass mechanism, albeit other scenarios exist [7].

Experiments searching for  $0\nu\beta\beta$  decay measure the summed energy spectrum of the final-state electrons searching for the distinctive signature of a peak at the  $Q$ -value of the decay ( $Q_{\beta\beta}$ ). To maximize sensitivity to this process,  $0\nu\beta\beta$  experiments must have a low background in the region of interest (ROI), good energy resolution at  $Q_{\beta\beta}$ , and a large active mass. There is currently a worldwide effort to search for  $0\nu\beta\beta$  with

several detector technologies and across a wide range of isotopes [8].

In this article, we present the results of a high-sensitivity search for the  $0\nu\beta\beta$  of  $^{130}\text{Te}$  to the ground state of  $^{130}\text{Xe}$  with a total exposure exceeding 2 tonne  $\cdot$  yr of  $\text{TeO}_2$  with CUORE data.

## 2. THE CUORE EXPERIMENT CHALLENGE

The Cryogenic Underground Observatory for Rare Events (CUORE) [9, 10] is a tonne-scale experiment located at the Laboratori Nazionali del Gran Sasso of INFN, Italy. It represents the culmination of a long chain of experiments based on cryogenic  $\text{TeO}_2$  calorimeters and covering almost 30 years of  $0\nu\beta\beta$  research [11].

The main scientific goal is the search for  $0\nu\beta\beta$  of  $^{130}\text{Te}$ , which benefits from a high natural isotopic abundance of  $(34.167 \pm 0.002)\%$  [12], and a large energy release of  $Q_{\beta\beta} = (2527.515 \pm 0.013)$  keV [13], placing the ROI above most natural  $\gamma$ -emitting radioactive backgrounds.

The CUORE detector is a close-packed array of 988  $^{\text{nat}}\text{TeO}_2$  crystals operated as cryogenic calorimeters, which can be cooled to temperatures as low as 7 mK [14]. They are arranged in a cylindrical structure of 19 identical copper-framed towers. Each tower hosts  $52.5 \times 5 \times 5$  cm<sup>3</sup> crystals divided into 13 floors of 4 crystals each. Every crystal has a mass of 750 g, corresponding to 742 kg of  $\text{TeO}_2$  and a total active mass of 206 kg of  $^{130}\text{Te}$ .

The towers are thermally connected to the mixing chamber of a multistage cryogen-free  $^3\text{He}/^4\text{He}$  dilution refrigerator uniquely designed for this application [14]. Precooling is made by five two-stage ( $\sim 40$  K and  $\sim 4$  K) pulse tube cryocoolers and a Joule-Thomson expansion valve. With an experimental volume of  $\sim 1$  m<sup>3</sup>, a mass of 1.5 tonnes at base temperature ( $\sim 10$ – $15$  mK), and a cooling power of  $4 \mu\text{W}$  at 10 mK, the CUORE cryostat is the largest, most powerful refrigerator system in operation. More details on the CUORE cryogenic system can be found in [14, 15]. To mitigate possible degradation in energy resolution due to vibrations, the detector is mechanically de-

coupled from the cryostat by means of a custom suspension system [14, 15].

Moreover, we actively tune the pulse tubes' relative phases to achieve the cancellation of vibrations at 1.4 Hz frequency and its harmonics [16].

When a particle interaction deposits energy inside a crystal, a neutron-transmutation-doped germanium thermistor [17] converts the thermal pulse into an electric signal. At CUORE operating temperatures,  $\text{TeO}_2$  crystals' specific heat yields a temperature increase of  $\sim 100 \mu\text{K}/\text{MeV}$  that corresponds to a voltage change of  $\sim 100 \mu\text{V}/\text{MeV}$ . A silicon heater [18] is used to inject reference pulses and achieve thermal gain stabilization [19].

Several steps are taken to protect CUORE from a background that could obscure a  $0\nu\beta\beta$  signal. The rock overburden shields the detectors from hadronic cosmic rays and reduces the muon flux by six orders of magnitude.

Two lead shields, 30-cm and 6-cm thick, at  $\sim 50\text{mK}$  above the detectors and  $\sim 4\text{K}$  around and below them suppress external  $\gamma$ -ray backgrounds. The lateral and lower shields are made of  $^{210}\text{Pb}$ -depleted ( $\lesssim 0.7\text{mBq kg}^{-1}$ ) ancient Roman lead [20]. Additional shielding from  $\gamma$  rays and neutrons is provided by an external lead shield (25-cm thick) surrounded by borated polyethylene and boric acid (20-cm thick). Finally, strict radio-purity material selection criteria and cleaning procedures were applied to all structures facing the detector [21].

Despite the technical complexity associated with operating such a large infrastructure, CUORE has been able to stably operate  $\geq 99.5\%$  of its 988 calorimeters over several years, cementing its place as the only successful tonne-scale milli-kelvin cryogenic calorimeter experiment not only in the field of  $0\nu\beta\beta$  decay but in general [22].

After the beginning of data taking in 2017, there have been two major interruptions of data collection, mainly to improve the cryogenic system performance and stability and install a new external calibration system with mixed  $^{232}\text{Th}$ - $^{60}\text{Co}$  sources. Since spring 2019, physics data collection has been ongoing steadily in stable temperature conditions at an average rate of  $50\text{ kg} \cdot \text{yr}/\text{month}$ .

### 3. THE SEARCH FOR $^{130}\text{Te}$ $0\nu\beta\beta$ DECAY

In this article, we present an analysis of the data collected between January 2021 and April 2023, corresponding to the second tonne  $\cdot \text{yr}$   $\text{TeO}_2$  exposure accumulated by CUORE [23]. The result of the preliminary combined  $^{130}\text{Te}$   $0\nu\beta\beta$  decay search with new data and the first tonne  $\cdot \text{yr}$   $\text{TeO}_2$  exposure [22] is presented at the end of this section.

The discussion on data processing that follows refers only to the second tonne  $\cdot \text{yr}$  data. Details on the data treatment and analysis employed for the first tonne  $\cdot \text{yr}$  are provided in [22].

The ultimate goal of our analysis chain is to convert the temperature changes in our calorimeters into an energy spectrum of events, which will allow us to look for evidence of  $0\nu\beta\beta$  decay in the ROI. To start, the voltage across each thermistor is amplified, filtered through a 6-pole Bessel filter, and continuously digitized with a sampling frequency of 1 kHz [24, 25]. During data acquisition, we save continuous detector waveforms that we digitally retrigger offline. For each triggered pulse, we analyze a 10-s window: 3s pretrigger serves as a proxy of the reference temperature before the interaction, while

we use the pulse amplitude to measure the energy released in the crystal.

We group our data into datasets covering one to two months each, bookended by calibration periods. We use the data between initial and final calibration to search for  $0\nu\beta\beta$  and refer collectively to them as *physics* data.

The main difference with respect to the last data release is the inclusion of a new multivariate noise cancellation algorithm, which we refer to as *offline denoising* [26]. The environmental noise is monitored by means of specially designed devices, including accelerometers, seismometers, microphones, and antennas, and a model of vibrational noise in thermal detectors is thereby constructed and used to mitigate its effect on CUORE calorimeters.

Denoised data are triggered with a low threshold trigger based on the optimum filter (OF) technique [27], which maximizes the signal-to-noise ratio by exploiting the distinct shapes of the stochastic noise power spectrum and the particle-induced signal spectrum. We build the OF transfer function for each calorimeter in each dataset and then extract the amplitude of triggered pulses from the maximum of the filtered waveforms.

Since the gain of a calorimeter depends on its temperature, we apply one of two algorithms to correct offline for possible time variations in the operating temperature of our detectors [28, 29]. The former uses monoenergetic heater pulses, and the latter uses the  $^{208}\text{Tl}$  events at 2615 keV from calibration and constitutes the default method for calorimeters with non-functioning or unstable pulser. For crystals in which both stabilizations are possible, we select the approach that yields the best energy resolution at the 2615 keV  $^{208}\text{Tl}$   $\gamma$  line in calibration data. We then calibrate our calorimeters in every dataset using the stabilized amplitude of the most intense  $\gamma$  lines in calibration. We fit the reconstructed peak positions against their energies using a second-order polynomial with zero intercepts [29].

To select  $0\nu\beta\beta$  candidate events, we apply the following selection criteria. First, we remove periods of time where the detector conditions were unstable or with unusually high noise levels. From Monte Carlo (MC) simulations, we expect that the majority of  $0\nu\beta\beta$  decays, namely,  $(88.350 \pm 0.090)\%$ , release all the energy into a single crystal [30]. The next step is hence to enforce an anti-coincidence (AC) veto by excluding any event that occurs within a  $\pm 5\text{ms}$  time window of another triggered event and has energy above 40 keV. Finally, we adopt a principal component analysis to perform a pulse shape discrimination (PSD) [22] and eliminate pile-up events, i.e., events with more than one energy deposit within the same time window, pulses with nonphysical shape, and excessively noisy pulses that survived basic data quality cuts.

To avoid biasing our results, we apply a simple salting procedure to blind our data in the ROI, shifting a random portion of events from the  $^{208}\text{Tl}$  line at 2615 keV in physics data down to the  $^{130}\text{Te}$   $Q$ -value at  $\sim 2528\text{keV}$  and vice versa. This generates an artificial peak at  $Q_{\beta\beta}$  with the shape of a true signal peak. We tune our analysis on blinded data and then undo the salting to extract final results on  $0\nu\beta\beta$  decay.

The signal detection efficiency is the product of several contributions: the containment efficiency, which we evaluate from MC as stated above, the reconstruction efficiency, the AC efficiency, and the PSD efficiency. The reconstruction efficiency is the probability that a signal event is triggered, has the energy reconstructed, and is not rejected because of basic data quality

cuts. This is measured using heater events and, given the large statistics available, is evaluated separately for each calorimeter and dataset and then averaged over the entire dataset. The anticoincidence efficiency is extracted by looking at the survival probability of fully absorbed  $\gamma$  events at 1460 keV from electron capture decays of  $^{40}\text{K}$ , which should be uncorrelated with any other events. Due to the low event rate in physics data, this term is computed as an average over the entire dataset. Lastly, the PSD efficiency is obtained as the average survival probability of events in the  $^{60}\text{Co}$ ,  $^{40}\text{K}$ , and  $^{208}\text{Tl}$   $\gamma$  peaks that survived the previous cuts. Again, given the limited statistics in physics data, we evaluate it over the entire dataset and extrapolate its value at  $Q_{\beta\beta}$ . The reconstruction efficiency varies between  $\sim 94.8$  and  $\sim 96\%$  depending on the dataset, while the average AC, PSD, and total analysis efficiency are 99.8%, 98.1%, and 93.1%, respectively [23].

We extract the detector response to a monoenergetic peak near  $Q_{\beta\beta}$  for each calorimeter in each dataset by fitting the high-statistics 2615 keV  $^{208}\text{Tl}$  line in calibration data [31]. We model it empirically as the superposition of three Gaussians with the same width to account for a slightly non-Gaussian behavior [31]. We obtain an exposure-weighted average FWHM of  $(7.43 \pm 0.37)$  keV at the 2615 keV calibration line [23]. To scale the energy resolution and calibration bias, defined as the difference between reconstructed and true peak position, at  $Q_{\beta\beta}$ , we fit the most prominent  $\gamma$  lines in physics data with the lineshape function extracted in calibration, letting both the peak position and energy resolution vary [32]. We parameterize the former as a linear function of energy and the latter as a quadratic function of energy [22]. The FWHM at  $Q_{\beta\beta}$  is  $(7.26^{+0.43}_{-0.47})$  keV and the energy bias  $\Delta E(Q_{\beta\beta})$  is  $(-0.11^{+0.19}_{-0.25})$  keV [23].

The CUORE physics spectrum around  $^{130}\text{Te}$   $Q$ -value after all selection cuts is shown in Figure 1.

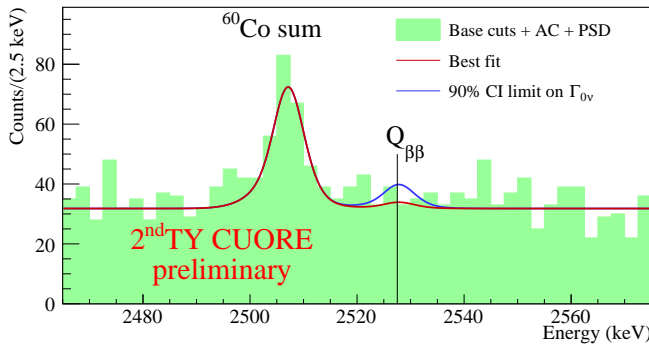


**FIGURE 1:** Physics spectrum for the second tonne  $\cdot$  yr  $\text{TeO}_2$  exposure in the ROI after all selection cuts, with the best-fit curve (solid red), the best-fit curve with the  $0\nu\beta\beta$  rate fixed to the 90% CI limit (solid blue) superimposed [23].

We model the region of interest (2465, 2575) keV with three components:

- (i) a posited peak at  $^{130}\text{Te}$   $Q_{\beta\beta}$  for the signal,
- (ii) the  $^{60}\text{Co}$  sum peak at 2505.7 keV due to  $\beta$  decays where both the 1173.2 keV and the 1332.5 keV deexcitation  $\gamma$  rays are fully absorbed in a single crystal,

- (iii) a flat background, mostly due to degraded  $\alpha$  particles ( $\sim 90\%$ ) and multi-Compton scattered 2615 keV  $\gamma$  rays ( $\sim 10\%$ ) from  $^{208}\text{Tl}$  [30, 32, 33].

We perform an unbinned Bayesian fit using the Bayesian Analysis Toolkit (BAT) [34]. The model parameters include the  $0\nu\beta\beta$  decay rate ( $\Gamma_{0\nu}$ ), a dataset-dependent background index (BI), the  $^{60}\text{Co}$  sum peak amplitude, and its position. We use a uniform prior for the signal rate and the BIs and restrict ourselves to nonnegative values of  $\Gamma_{0\nu}$ .

We find no evidence for  $0\nu\beta\beta$  decay and set a limit on the  $^{130}\text{Te}$   $0\nu\beta\beta$  half-life of  $T_{1/2}^{0\nu} > 2.7 \cdot 10^{25}$  yr with a 90% credibility interval (CI) [23]. Repeating the fit without the  $0\nu\beta\beta$  contribution, we measure an average BI at  $Q_{\beta\beta}$  of  $(1.30 \pm 0.03) \cdot 10^{-2}$  counts/(keV kg yr) [23]. Based on the background-only fit of the data, we generate  $10^4$  pseudo-experiments populated with only the  $^{60}\text{Co}$  and background components. Fitting them with the signal-plus-background model, we extract our median exclusion sensitivity,  $T_{1/2}^{0\nu} = 3.1 \cdot 10^{25}$  yr (90% CI) [23].

Combining the second tonne  $\cdot$  yr data discussed so far with the first tonne  $\cdot$  yr data analyzed in [22], we obtain an overall exposure of 2023 kg  $\cdot$  yr of  $\text{TeO}_2$ . There is no evidence for  $0\nu\beta\beta$ , and we set a 90% CI limit on the  $^{130}\text{Te}$   $0\nu\beta\beta$  decay rate of  $\Gamma_{0\nu} < 2.1 \cdot 10^{-26}$  yr $^{-1}$  [23]. The corresponding limit on the  $^{130}\text{Te}$  half-life for  $0\nu\beta\beta$  decay is  $T_{1/2}^{0\nu} > 3.3 \cdot 10^{25}$  yr (90% CI) [23].

Assuming  $0\nu\beta\beta$  decay is mediated by light Majorana neutrino exchange, our combined limit on the  $^{130}\text{Te}$   $0\nu\beta\beta$  decay half-life corresponds to a preliminary upper limit of 75–255 meV on the effective Majorana mass  $m_{\beta\beta}$  [23], where the spread is induced by different nuclear matrix element calculations [35, 36, 37, 38, 39, 40, 41].

The next steps that we anticipate toward the final 2 tonne  $\cdot$  yr analysis include reprocessing the first tonne  $\cdot$  yr with the new analysis chain, repeating the  $0\nu\beta\beta$  decay fit on the entire CUORE statistics, and finalizing the study of systematic effects.

## 4. OTHER ANALYSES WITH CUORE

As stated above, the primary goal of the CUORE experiment is the search for  $0\nu\beta\beta$  decay of  $^{130}\text{Te}$  to the ground state of  $^{130}\text{Xe}$  [9, 10]. However, the search for the double beta decay of  $^{130}\text{Te}$  to the first  $0^+$  excited state of  $^{130}\text{Xe}$  is also among CUORE targets. An analysis of the  $0\nu\beta\beta$  mode as well as the Standard Model allowed counterpart,  $2\nu\beta\beta$ , has been performed with the data acquired between May 2017 and July 2019, corresponding to a total  $\text{TeO}_2$  exposure of 372.5 kg  $\cdot$  yr [42]. No significant evidence of either decay was observed, and a Bayesian lower limit on the half-lives was extracted [42]:  $T_{1/2}^{0\nu} > 5.9 \cdot 10^{24}$  yr (90% CI) and  $T_{1/2}^{2\nu} > 1.3 \cdot 10^{24}$  yr (90% CI) on the  $0\nu$  mode and on  $2\nu$  mode, respectively.

Moreover, with a total exposure of 300.7 kg  $\cdot$  yr, we made the most precise measurement of  $^{130}\text{Te}$   $2\nu\beta\beta$  half-life to date:  $T_{1/2}^{2\nu} = 8.76^{+0.09}_{-0.07}(\text{stat})^{+0.14}_{-0.17}(\text{syst}) \cdot 10^{20}$  yr [30]. Since mitigating the experimental background is a key requirement to increase our sensitivity to  $0\nu\beta\beta$  and toward the next generation experiment, CUPID [43], precise modeling of the entire energy spectrum is essential to understand the data we are collecting and minimize residual backgrounds in the region of interest. A detailed background model of CUORE is in preparation [44] with roughly a threefold increase in the analyzed exposure compared to [30].

The use of tellurium with natural isotopic composition allows us to search for other rare decays, such as double beta decay in  $^{128}\text{Te}$  [45] and  $^{120}\text{Te}$  [46].

The first limit on  $0\nu\beta\beta$  half-life of  $^{128}\text{Te}$  with CUORE data is presented in [45]. With a  $309.3 \text{ kg} \cdot \text{yr}$   $\text{TeO}_2$  exposure, we found no evidence of  $0\nu\beta\beta$  decay and set a Bayesian lower limit on the half-life of this isotope,  $T_{1/2}^{0\nu} > 3.6 \cdot 10^{24} \text{ yr}$  (90% CI) [45]. Improving by a factor over 30 the previous direct searches, this result represents the most stringent limit on the  $0\nu\beta\beta$  half-life of  $^{128}\text{Te}$  [45].

Exploiting its extremely clear decay signature due to the presence of a positron in the final state, we performed an initial search for  $0\nu\beta^+\text{EC}$  decay in  $^{120}\text{Te}$  analyzing  $372.5 \text{ kg} \cdot \text{yr}$   $\text{TeO}_2$  exposure [46]. No evidence of such a signal was observed, and a 90% CI Bayesian lower limit of  $2.9 \cdot 10^{22} \text{ yr}$  was set on  $^{120}\text{Te}$  half-life for this decay, improving by an order of magnitude the existing limit from CUORE-0 and Cuoricino [46].

Interesting analyses making use of CUORE data extend beyond double beta decay [33]. Among them, we developed a comprehensive thermal model of CUORE [47], which is paramount to the improvement of CUORE detector performance as well as to the optimization of the detector response in the CUPID experiment. Furthermore, we are finalizing a study of how the marine microseismic activity of the Mediterranean Sea affects our detector response [48]. The analysis is based on a multi-detector approach, involving data from Copernicus Marine Environment Monitoring Service (CMEMS), seismometers, and the CUORE bolometers [48]. Finally, analyses in the low energy regime exploiting the large accumulated exposure paired with the low energy thresholds of CUORE calorimeters are in progress [33, 49].

## 5. CONCLUSIONS AND PERSPECTIVES

CUORE is the first experiment to demonstrate the stable operation of a tonne-scale mill-kelvin cryogenic calorimeter while maintaining extremely low radioactive backgrounds [22]. So far, we have exceeded 2 tonne  $\cdot \text{yr}$   $\text{TeO}_2$  analyzed exposure and data collection is proceeding smoothly toward our target of 3 tonne  $\cdot \text{yr}$   $\text{TeO}_2$  (1 tonne  $\cdot \text{yr}$   $^{130}\text{Te}$ ) exposure.

With 2023  $\text{kg} \cdot \text{yr}$   $\text{TeO}_2$  exposure, obtained by combining the data analyzed in [22] with newly acquired ones, we found no evidence of  $0\nu\beta\beta$  and set a Bayesian lower limit of  $3.3 \cdot 10^{25} \text{ yr}$  (90% CI) on  $^{130}\text{Te}$  half-life for such decay.

CUORE physics program is rich and includes the analysis of many  $\beta\beta$  decays [42, 45, 46] as well as searches for new physics in the low energy regime [33, 48] and several thermal detector noise studies [26, 48].

Looking to the future, CUORE will continue to collect data until the next generation experiment CUPID [43] begins its commissioning. Since the same technology and cryogenic infrastructure will be used, CUORE results represent important feedback for the CUPID project, for both the cryogenic system and background budget [44].

## CONFLICTS OF INTEREST

The authors declare no conflicts of interest. Correspondence and requests for material should be addressed to the CUORE Collaboration ([cuore-spokeperson@lngs.infn.it](mailto:cuore-spokeperson@lngs.infn.it)).

## ACKNOWLEDGMENTS

The CUORE Collaboration thanks the directors and staff of the Laboratori Nazionali del Gran Sasso and the technical staff of our laboratories. This work was supported by the Istituto Nazionale di Fisica Nucleare (INFN); the National Science Foundation under Grant Nos. NSF-PHY-0605119, NSF-PHY-0500337, NSF-PHY-0855314, NSF-PHY-0902171, NSF-PHY-0969852, NSF-PHY-1614611, NSF-PHY-1307204, NSF-PHY-1314881, NSF-PHY-1401832, and NSF-PHY-1913374; and Yale University. This material is also based upon work supported by the US Department of Energy (DOE) Office of Science under Contract Nos. DE-AC02-05CH11231 and DE-AC52-07NA27344; by the DOE Office of Science, Office of Nuclear Physics under Contract Nos. DE-FG02-08ER41551, DE-FG03-00ER41138, DE-SC0012654, DE-SC0020423, DE-SC0019316; and by the EU Horizon2020 research and innovation program under the Marie Skłodowska-Curie Grant Agreement No. 754496. This research used resources of the National Energy Research Scientific Computing Center (NERSC). This work makes use of both the DIANA data analysis and APOLLO data acquisition software packages, which were developed by the CUORICINO, CUORE, LUCIFER and CUPID-0 Collaborations.

## References

- [1] R. L. Workman et al. (Particle Data Group), *Prog. Theor. Exp. Phys.* **2022**, 083C01 (2022) and 2023 update.
- [2] E. Majorana, *Nuovo Cimento* **14**, 171 (1937).
- [3] M. Fukugita and T. Yanagida, *Phys. Lett. B* **174**, 45–47 (1986).
- [4] J. Schechter and J. W. F. Valle, *Phys. Rev. D* **25**, 2951 (1982).
- [5] S. M. Bilenky, *Eur. Phys. J. H* **38** 345 (2013).
- [6] P. Fileviez Perez, Pavel, C. Murgui and A. D. Plascencia, *Phys. Rev. D* **104**, 055007 (2021).
- [7] R. N. Mohapatra and P. B. Pal, *World Sci. Lect. Notes Phys.* **41** (1991).
- [8] M. Agostini, G. Benato, J. A. Detwiler, J. Menéndez, and F. Vissani, *Rev. Mod. Phys.* **95**, 025002 (2023).
- [9] C. Arnaboldi et al. (CUORE Collaboration), *Nucl. Instrum. Meth. A* **518**, 775–798 (2004).
- [10] D. R. Artusa et al. (CUORE Collaboration), *Adv. High Energy Phys.* **879871** (2015).
- [11] C. Brofferio and S. Dell’Oro, *Rev. Sci. Instrum.* **89**, 121502 (2018).
- [12] M. A. Fehr, M. Rehkemper, and A. N. Halliday, *Int. J. Mass Spectroscopy* **232**, 83 (2004).
- [13] S. Rahaman, V. V. Elomaa, T. Eronen, J. Hakala, A. Jokinen, A. Kankainen, J. Rissanen, J. Suhonen, C. Weber, and J. Äystö, *Phys. Rev. Lett. B* **703**, 412 (2011).
- [14] C. Alduino et al. (CUORE Collaboration), *Cryogenics* **92**, 9–21 (2019).
- [15] D. Q. Adams et al. (CUORE Collaboration), *Prog. Part. Nucl. Phys.* **122**, 103902 (2022).
- [16] A. D. Addabbo et al., *Cryogenics* **93**, 56–65 (2018).
- [17] E. E. Haller, N. P. Palaio, M. Rodder, W. L. Hansen and E. Kreysa, *NTD Germanium: A Novel Material for Low Temperature Bolometers*, 21–36 (Springer US, Boston, MA) (1984).
- [18] E. Andreotti et al., *Nucl. Instrum. Meth. A* **664**, 161–170 (2012).
- [19] K. Alfonso et al., *J. Instrum.* **13**, P02029 (2018).
- [20] L. Pattavina et al., *Eur. Phys. J. A* **55**, 127 (2019).

- [21] F. Alessandria et al. (CUORE Collaboration), *Astropart. Phys.* **45**, 13–22 (2013).
- [22] D. Q. Adams et al. (CUORE Collaboration), *Nature* **604** (7904), 53 (2022).
- [23] K. Alfonso, PoS (TAUP 2023) **155** (2023).
- [24] C. Arnaboldi, P. Carniti, L. Cassina, C. Gotti, X. Liu, M. Maino, G. Pessina, C. Rosenfeld and B. Zhu, *J. Instrum.* **13**, P02026 (2018).
- [25] S. Di Domizio, A. Branca, A. Caminata, L. Canonica, S. Copello, A. Giachero, E. Guardincerri, L. Marini, M. Pallavicini and M. Vignati, *J. Instrum* **13**, P12003 (2018).
- [26] K. Vetter, PoS (TAUP 2023) **293** (2023).
- [27] S. Di Domizio, F. Orio and M. Vignati, *J. Instrum* **6**, P02007 (2011).
- [28] A. Alessandrello et al., *Nucl. Instrum. Meth. A* **412**, 454 (1998).
- [29] C. Alduino et al. (CUORE Collaboration), *Phys. Rev. C* **93**, 045503 (2016).
- [30] D. Q. Adams et al. (CUORE Collaboration), *Phys. Rev. Lett.* **131**, 249902 (2023).
- [31] C. Alduino et al. (CUORE Collaboration), *Phys. Rev. Lett.*, **120**, 132501 (2018).
- [32] D. Q. Adams et al. (CUORE Collaboration), *Phys. Rev. Lett.* **124**, 122501 (2020).
- [33] C. Alduino et al. (CUORE Collaboration), *Eur. Phys. J. C* **77**, 12 857 (2017).
- [34] A. Caldwell, D. Kollár and K. Kröninger, *Computer Physics Communications* **180**, 2197 (2009).
- [35] J. Menéndez et al., *Nucl. Phys. A* **818**, 139–151 (2009).
- [36] F. Šimkovic et al., *Phys. Rev. C* **87**, 045501 (2013).
- [37] N. López Vaquero, T. R. Rodríguez, and J. L. Egido, *Phys. Rev. Lett.* **111**, 142501 (2013).
- [38] A. Neacsu, and M. Horoi, *Phys. Rev. C* **91**, 024309 (2015).
- [39] J. M. Yao et al., *Phys. Rev. C* **91**, 024316 (2015).
- [40] J. Barea, J. Kotila, and F. Iachello, *Phys. Rev. C* **91**, 034304 (2015).
- [41] J. Hyvärinen, and J. Suhonen, *Phys. Rev. C* **91**, 024613 (2015).
- [42] D.Q. Adams et al. (CUORE Collaboration), *Eur. Phys. J. C* **81**, 567 (2021).
- [43] W. R. Armstrong et al. (CUPID Collaboration), arXiv:1907.09376 (2019).
- [44] S. Ghislandi, PoS (TAUP 2023) **174** (2023).
- [45] D. Q. Adams et al. (CUORE Collaboration), *Phys. Rev. Lett.* **129**, 22 222501 (2022).
- [46] D. Q. Adams et al. (CUORE Collaboration), *Phys. Rev. C* **105**, 065504 (2022).
- [47] D.Q. Adams et al. (CUORE Collaboration), *JINST* **17** P11023 (2022).
- [48] S. Quitadamo, PoS (TAUP 2023) **282** (2023).
- [49] A. Ressa, PoS (TAUP 2023) **090** (2023).